Res. Chem. Intermed., Vol. 21, No. 6, pp. 577-586 (1995).
© VSP 1995

WHY IS THE Si–X STRETCHING FREQUENCY OF $X_8Si_8O_{12}$ (X = H, CH_3, Cl) MUCH HIGHER THAN THAT OF $XSi(OSiME_3)_3$?

M. BÄRTSCH, G. CALZAFERRI* and C. MARCOLLI
Institute for Inorganic and Physical Chemistry, University of Berne, Freiestrasse 3, CH-3000 Bern 9, Switzerland

Received 2 June 1994; accepted 4 November 1994

Abstract--The totally symmetric stretching frequencies υ_s(Si–X) of the octasilases-quioxanes $X_8Si_8O_{12}$ are distinctively larger than those of $XSi(OSiMe_3)_3$ for X = H, CH_3, Cl whereas υ_s(Si–H) of $H_8Si_8O_{12}$ and of $H_{10}Si_{10}O_{15}$ differ very little. Inspection of the experimental data and molecular orbital calculations of the EHMO-ASED type show that this striking discrepancy is caused by the differences in the X–Si–O–Si conformations. The cage structure of $X_8Si_8O_{12}$ requires the anti X–Si–O–Si conformation whereas the syn conformation is the stable one in $XSi(OSiMe_3)_3$. The Si–H bond order decreases from anti to syn caused by a decreasing interaction of the H-1s orbital with the Si–O-pπ type orbitals.

INTRODUCTION

We have observed that the totally symmetric stretching frequencies υ_s(Si–X) of $X_8Si_8O_{12}$, **1**, are distinctively larger than those of $XSi(OSiMe_3)_3$, **2**, for X = H, CH_3, Cl, and that especially Si–H vibrates at about 100 cm^{-1} higher frequency than in all methylsilyl compounds investigated by McKean *et al.* [1]. An obvious difference between these two types of molecules is the cage structure of **1** and the open framework of **2**, as illustrated in Figures 1 and 2. The question arises, whether the cage structure of **1** is responsible for the observed shift of υ_s(Si–X) towards higher energy, because it allows only an anti X–Si–O–Si conformation, while the open structure **2** can in principle exist as anti and as syn.

The crystal structure of $H_8Si_8O_{12}$ has lately been reinvestigated [2], its electronic structure is well understood [3], and detailed spectroscopic studies accompanied by normal coordinate analysis have been carried out recently [4,5]. The Si–H stretching modes appear in a spectral region sparsely populated by other fundamentals and we know that coupling with other modes is small for both, $H_8Si_8O_{12}$ and $HSi(OSiMe_3)_3$. This means that any change in the Si–H stretching frequency is reflected by the Si–H force constant. We therefore focus our special attention on this case. Empirical correlation of the Si–H stretching frequency of $R_1R_2R_3SiH$ compounds with electronegativity properties of a large

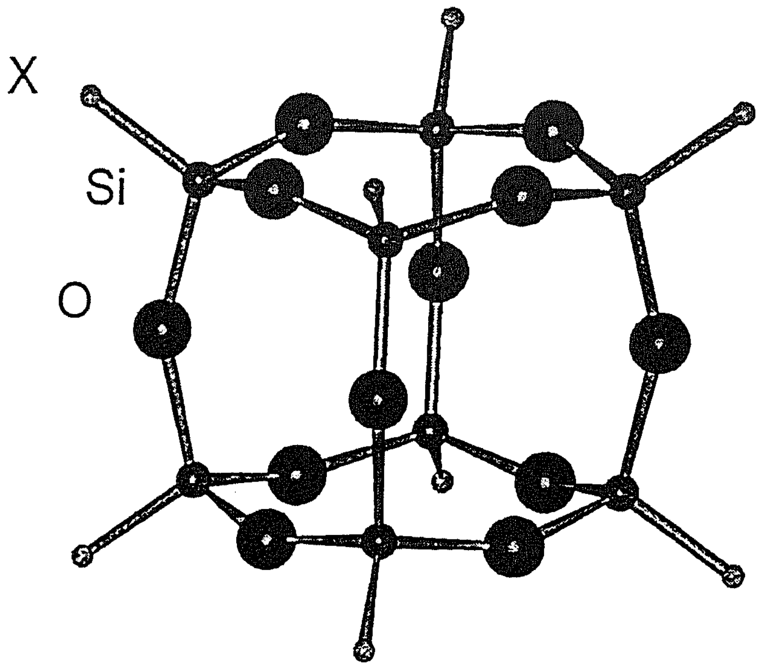

Figure 1. Structure of the $X_8Si_8O_{12}$ molecule.

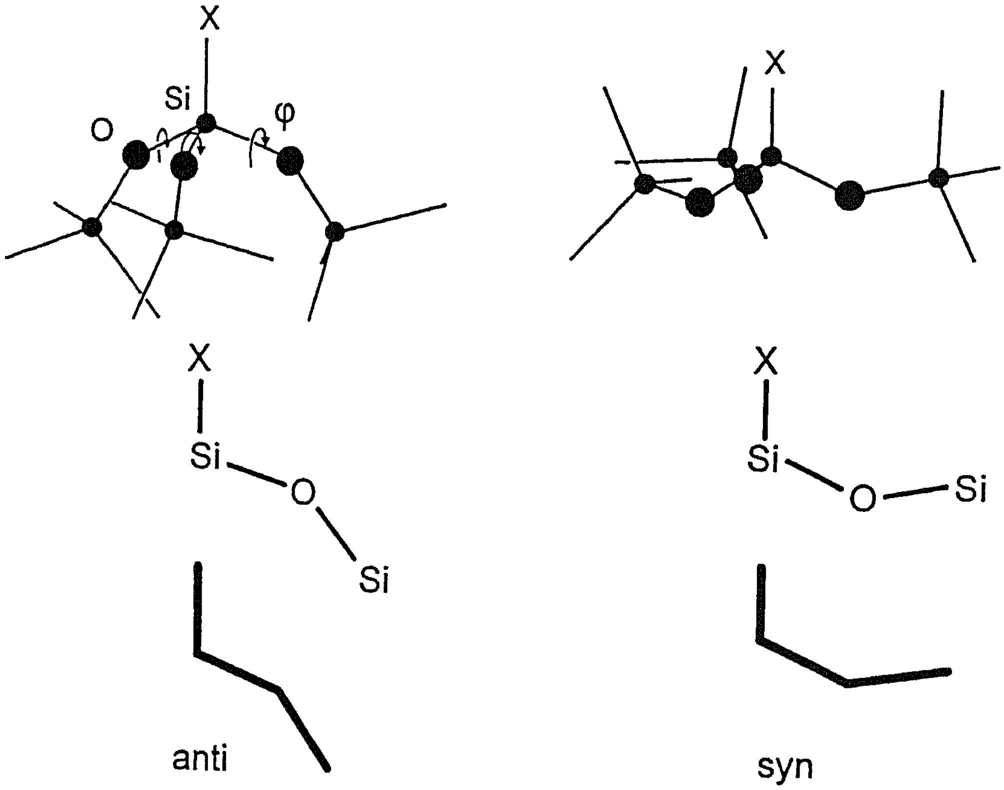

Figure 2. Anti ($\varphi = 0°$) and syn ($\varphi = 180°$) conformation of $XSi(OSiMe_3)_3$.

number of substituents R_1, R_2, and R_3 has been discussed some years ago and remarkable agreement between predicted and observed data has been reported [6]. Using a few selected compounds as standards, the authors were able to derive a characteristic constant for each group such that the Si–H frequency of other substituted silanes and siloxanes can be well predicted, provided the spectra have been measured under the same conditions, *e.g.* in the same solvent. This approach, however, does not work for the totally symmetric Si–H stretching vibration of $H_8Si_8O_{12}$ and the same is true for $H_{10}Si_{10}O_{15}$, the crystal structure of which has been investigated in detail lately [7]. What is the reason for this deviation? This question becomes increasingly relevant as the number of substituted spherosiloxanes $RH_7Si_8O_{12}$ [8], $RR'H_6Si_8O_{12}$ [9], of other similar molecules [10] and applications of T8-hydrospherosiloxanes [11] are growing.

The υ(Si–C) and υ(Si–Cl) stretching vibrations absorb in a spectral region where vibrational coupling with modes of the neighboring groups can no longer be neglected. We will show, however, that the same mechanism responsible for the shift of the totally symmetric Si–H stretching frequency from **1** to **2** has to be considered also in these two cases.

RESULTS AND DISCUSSION

The Si–X stretching frequencies of $X_8Si_8O_{12}$, $XSi(OSiMe_3)_3$, $HSi(OSiMe_2H)_3$, and $H_{10}Si_{10}O_{15}$ are listed in Table 1. In all these compounds, the silicon atom involved in the Si–X stretching vibration is coordinated by three oxygens which form a bridge to the next silicon atoms. In spite of the very similar coordination, the stretching frequency rises significantly from the open framework to the cage structure where it exceeds the normal region distinctly. In the case of X = CH_3 and Cl vibrational coupling with other modes influences υ_s(Si–X), while the only parameter which affects υ_s(Si–H) significantly is the Si–H stretching force constant [5]. We therefore expect a smaller Si–H bond order for **2** than for **1**. To find out what factors are responsible for the observed shift of υ_s(Si–H) towards higher energy, we have calculated the Si–X bond order and the energy of $XSi(OSiMe_3)_3$ for different dihedral angles from $\varphi = 0°$, where geometry optimization has been carried out, to 180°. The results obtained for $HSi(OSiMe_3)_3$ are shown in Figure 3 where we see that the Si–H bond order drops between $\varphi = 0°$ and 120° and then remains nearly constant. We also note that the anti conformation of this molecule is not stable with respect to syn, due to strong steric interactions between the methyl groups for small values of φ, caused by orbital interactions (D) and core-core repulsion (C). No possibility was found to arrange the methyl groups in a favourable way to avoid significant repulsion. This means that only conformers with a large angle φ need to be considered for these molecules. In Table 2 we therefore compare the Si–X bond orders of different syn-$XSi(OSiMe_3)_3$ molecules with the bond orders of the corresponding $X_8Si_8O_{12}$ which are, of course, anti.

The result is very clear. The Si–X bond orders of the $X_8Si_8O_{12}$ molecules are considerably larger than those of the syn-$XSi(OSiMe_3)_3$. This strongly points to significant syn-anti influence on the Si–H stretching force constant f_R. In fact normal coordinate analysis not reported here shows that f_R drops from 3.24 mdyn/Å for $H_8Si_8O_{12}$ [5] by about 8% for the syn conformation, in good agreement with the drop of the bond order illustrated in Figure 3, curve B. We note that the Si_X–O bond order is much less affected by the different environment. To further clarify the factor responsible for the bond order decrease from anti to syn, all methyl groups in $XSi(OSiMe_3)_3$ were replaced by hydroxy groups and

Table 1.
Experimental FT-Raman Si-X stretching frequencies/cm^{-1}.

Molecule	X=H	X=CH$_3$	X=Cl
$X_8Si_8O_{12}$ [a]	2302	819	733
$XSi(OSiMe_3)_3$	2207	748[d]	588
$XSi(OSiMe_2H)_3$	2223[b]/2214[c]		
$X_{10}Si_{10}O_{15}$[a]	2293		

[a] Totally symmetric stretching vibration.
[b] Reference [6].
[c] Reference [12].
[d] Assignment according to Reference [12].

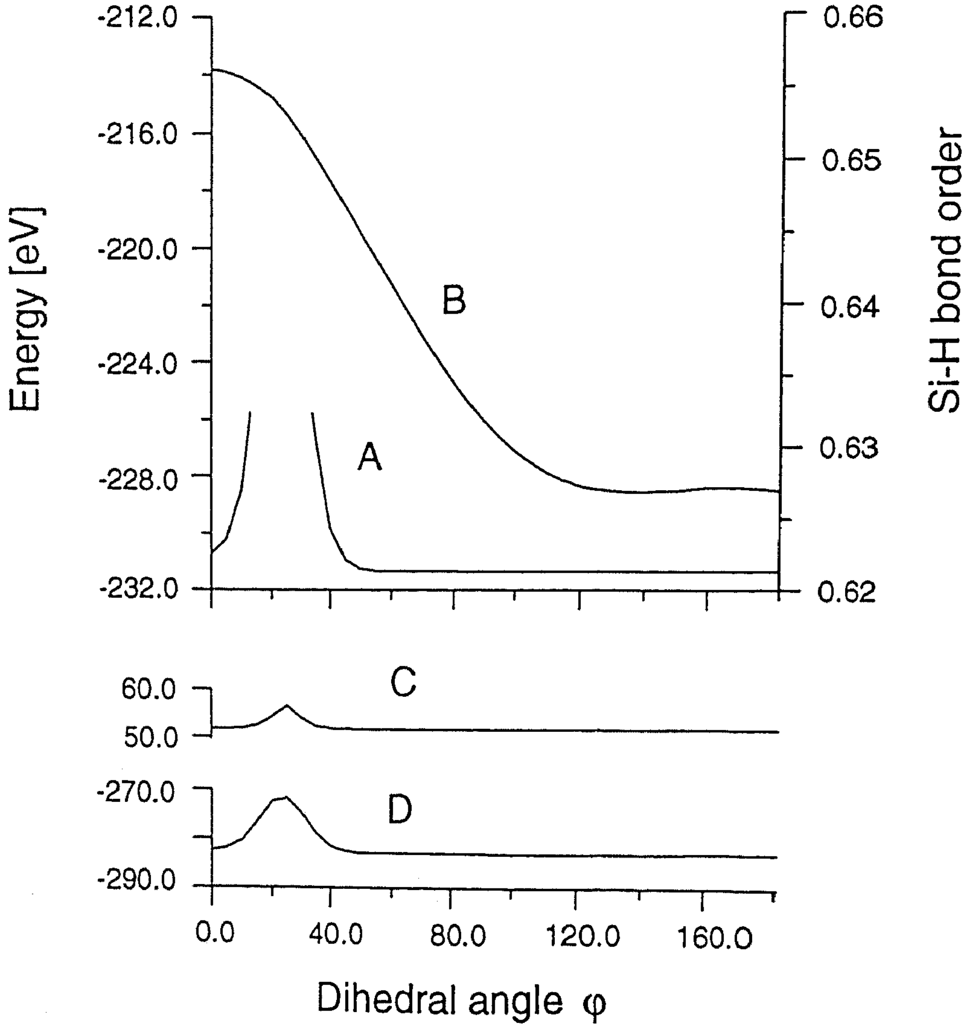

Figure 3. Energies and bond order of $HSi(OSiMe_3)_3$ as a function of the dihedral angle φ; A: total energy E_{tot}, B: Si–H bond order, C: core-core repulsion E_{Rep}, D: extended-Hückel binding energy ΔE_{EHMO}. The barrier at about 30° is enormous and is caused by orbital interactions (D) and core-core repulsion (C). We have not searched for a minimum pathway.

Table 2.
Bond order.

	$X_8Si_8O_{12}$ $\varphi = 0°$	$XSi(OSiMe_3)_3$ $\varphi = 180°$	$XSi(OSi(OH)_3)_3$ $\varphi = 0°$	$XSi(OSi(OH)_3)_3$ $\varphi = 180°$
X = H				
Si–H	0.654	0.626	0.656	0.625
Si_H–O	0.665	0.671	0.664	0.671
Si–O	0.665	0.714	0.677	0.677
X = CH_3				
Si–C	0.587	0.567	0.588	0.566
Si_C–O	0.664	0.670	0.664	0.670
Si–O	0.664	0.714	0.677	0.677
X = Cl				
Si–Cl	0.702	0.688	0.704	0.687
Si_{Cl}–O	0.656	0.660	0.655	0.660
Si–O	0.656	0.714	0.678	0.677

we have carried out the same calculations as before. The results obtained are listed in the third and fourth column of Table 2. They show that the Si–X bond order is scarcely affected by this replacement, which means that the Si–X bond order depends significantly on the conformation. We note that also the Si_X–O bond orders behave very similarly in both cases. The data reported in Table 3 show that the charge on the substituent X is in all cases a little larger for syn with respect to anti and almost the same on the adjacent Si atom, so that the change in polarity of the Si–X bond appears to be of minor importance. The charges on the oxygen atoms differ, however, significantly between $XSi(OSiMe_3)_3$ and $X_8Si_8O_{12}$ while the syn and anti isomers of $XSi(OSi(OH)_3)_3$ show negligible differences. This means that the charge differences in the former case are not dominated by the conformation but by the substituents.

We now compare $HSi(OSiMe_3)_3$ with $HSi(OSiMe_2H)_3$ because in this molecule free or nearly free rotation around the dihedral angle is expected. This is reflected in curve A of Figure 4. From our previous arguments we therefore expect a higher Si–H stretching frequency than that of $HSi(OSiMe_3)_3$, but lower than that of $H_8Si_8O_{12}$. For $H_{10}Si_{10}O_{15}$ we expect that υ_s(Si–H) should appear at approximately the same frequency as in the case of $H_8Si_8O_{12}$. Both expectations are in agreement with the experimental values reported in Table 1. This further supports our conclusion that the unusually large totally symmetric stretching frequency υ_s(Si–X) of $X_8Si_8O_{12}$, with respect to $XSi(OSiMe_3)_3$, is caused by the different X–Si–O–Si conformation of these two types of molecules.

The reason for the change in bond order from anti ($\varphi = 0°$) to syn ($\varphi = 180°$) can be understood by investigating the molecular orbitals responsible for the Si–H bond. It is sufficient to do this for the $HSiOSi(OH)_3$ fragment which represents one third of the total bond order change observed for $HSi(OSi(OH)_3)_3$, as illustrated in Figure 5. In Figure 6 we

Table 3.
Charge /$1.6 \cdot 10^{-19}$ C.

	$X_8Si_8O_{12}$ $\varphi = 0°$	$XSi(OSiMe_3)_3$ $\varphi = 180°$	$XSi(OSi(OH)_3)_3$ $\varphi = 0°$	 $\varphi = 180°$
X = H				
H	-0.069	-0.093	-0.068	-0.094
Si_H	0.464	0.462	0.461	0.467
O	-0.263	-0.204	-0.264	-0.258
Si	0.464	0.025	0.598	0.598
X = CH_3				
C	-0.010	-0.042	-0.008	-0.046
Si_C	0.422	0.428	0.422	0.433
O	-0.276	-0.211	-0.270	-0.264
Si	0.422	0.025	0.596	0.598
X = Cl				
Cl	-0.176	-0.186	-0.175	-0.186
Si_{Cl}	0.693	0.694	0.696	0.698
O	-0.345	-0.249	-0.303	-0.303
Si	0.693	0.025	0.596	0.598

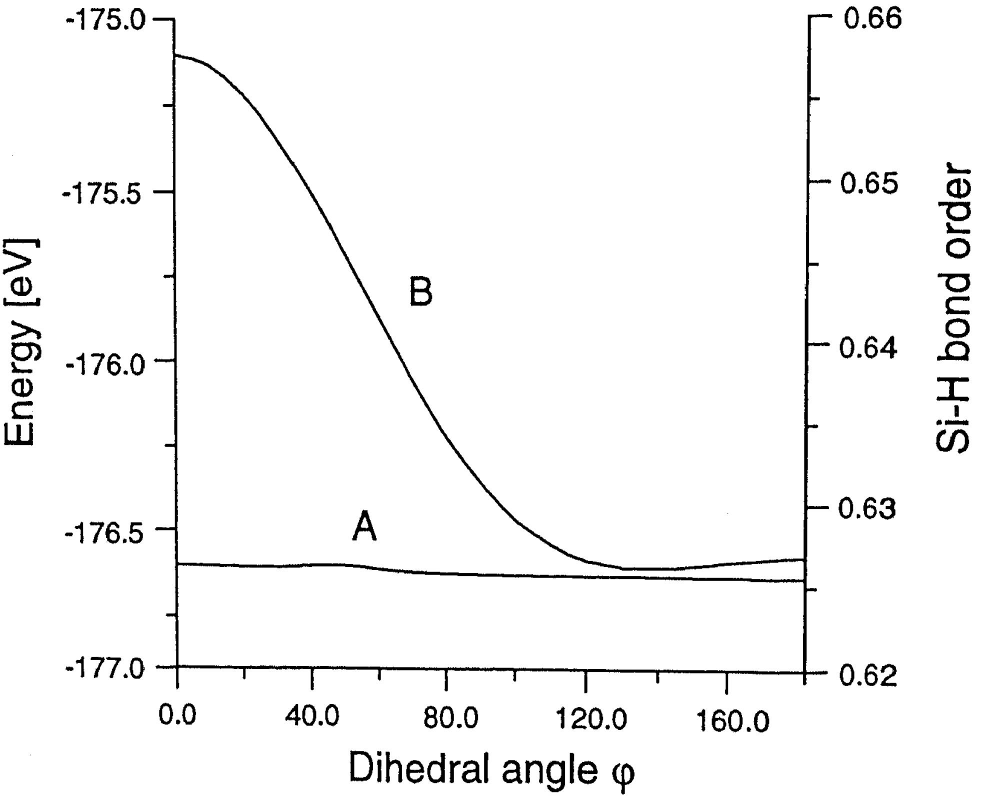

Figure 4. Total energy E_{tot} (A) and Si–H bond order (B) of $HSi(OSiMe_2H)_3$ as a function of the dihedral angle φ.

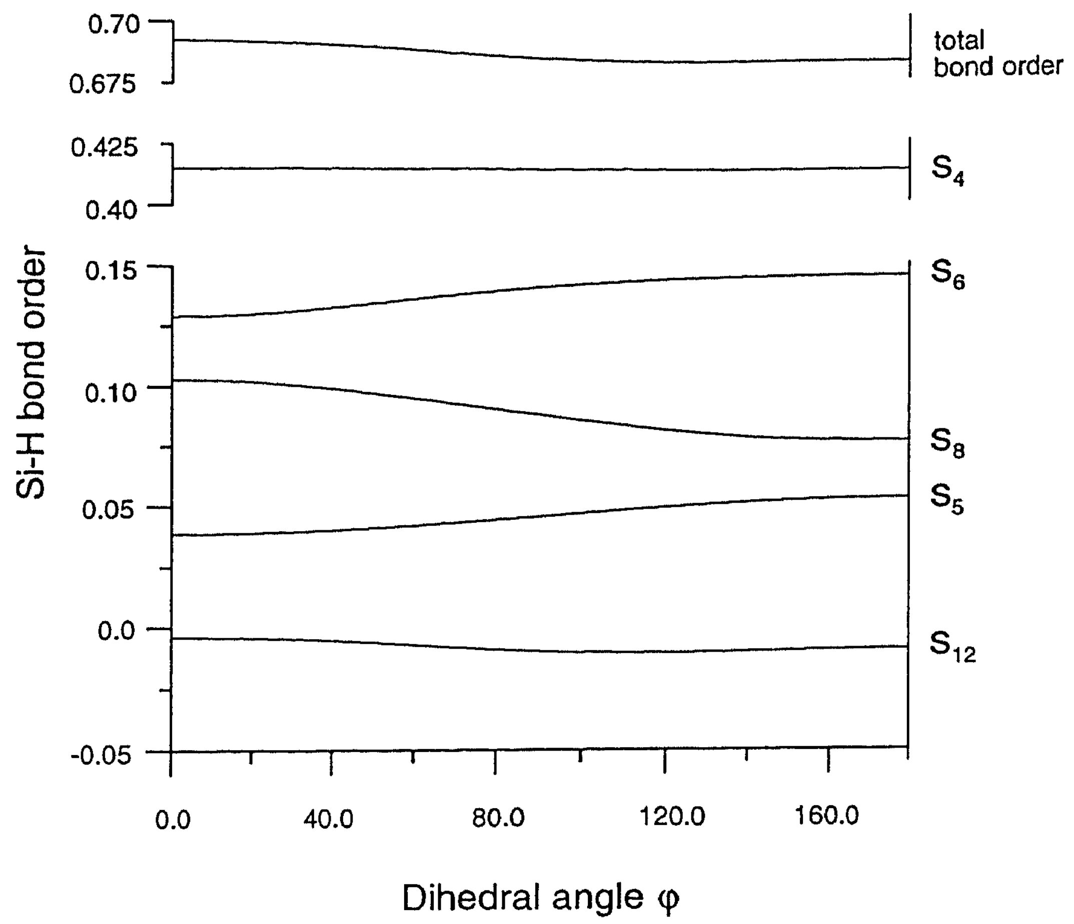

Figure 5. Total and individual Si–H bond orders of the molecular orbitals of the $HSiOSi(OH)_3$ fragment as a function of the dihedral angle φ. The change in the total Si–H bond order between anti ($\varphi = 0°$) and syn ($\varphi = 180°$) of this fragment is one third of the change observed for $HSi(OSi(OH)_3)_3$.

show the correlation diagram H + $SiOSi(OH)_3 \rightarrow HSiOSi(OH)_3$ for both the anti and the syn conformations to illustrate the Si–H interaction. From these two figures it is obvious that the main contribution to the Si–H bond comes from S_4 which represents the Si-3s + H-1s sσ-interaction and which is independent of the dihedral angle φ. Furthermore, the form of the two $SiOSi(OH)_3$ σ-orbitals S_5 and S_7 is such that their angle dependence of the interaction with the H-1s atom orbital is small and not dominant. What remains is the Si–O-pπ orbital S_8 which by nature shows an angle dependence [13]. The individual bond order change of S_8 is indeed dominant and this is even more pronounced in the whole molecule $HSi(OSi(OH)_3)_3$.

EXPERIMENTAL

The FT-Raman spectra were recorded on a BOMEM DA3.01 FTIR spectrometer. A Quantronix 114 cw-Nd:YAG laser was used as excitation source operating in single TEM_{00} mode at 9394.5 cm^{-1}. The spectra were measured with a liquid nitrogen cooled InGaAs detector using a quartz beamsplitter. $H_8Si_8O_{12}$, $H_{10}Si_{10}O_{15}$, $Me_8Si_8O_{12}$, and $Cl_8Si_8O_{12}$ were

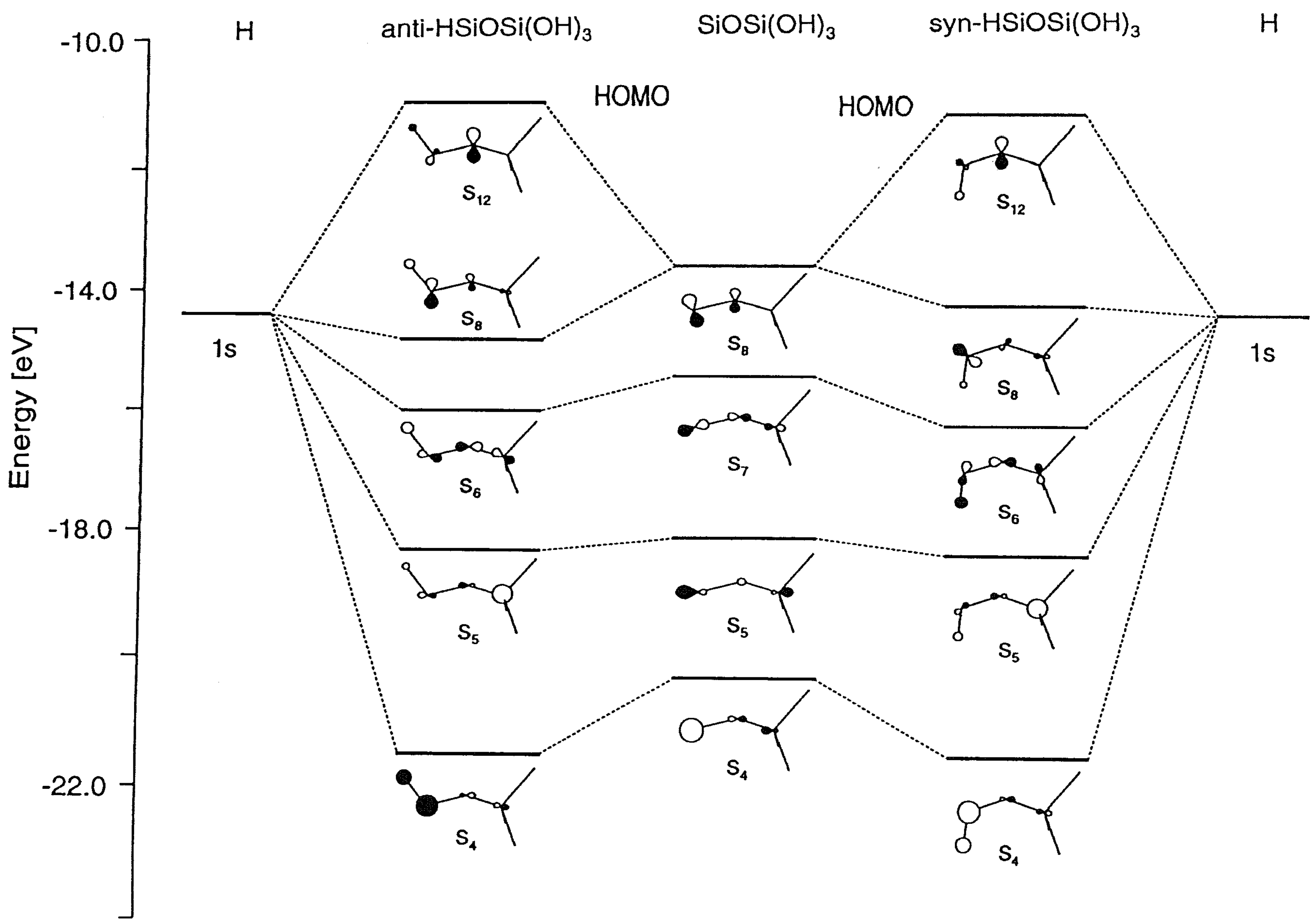

Figure 6. Correlation diagram H + $SiOSi(OH)_3$ → $HSiOSi(OH)_3$. Left: anti-$HSiOSi(OH)_3$. Right: syn-$HSiOSi(OH)_3$.

synthesized according to [14-16], and measured as crystalline powders. $H_{10}Si_{10}O_{15}$ was purified as described in Reference [17]. Because of its reactivity with humidity $Cl_8Si_8O_{12}$ had to be sealed in a Duran capillary tube. $HSi(OSiMe_3)_3$, $MeSi(OSiMe_3)_3$, and $ClSi(OSiMe_3)_3$ were used as purchased from ABCR (Karlsruhe, Germany) and measured as neat liquids at ambient temperature.

Molecular orbital calculations were carried out by the extended-Hückel method [18] and Mulliken population analysis was applied [19]. The off-diagonal elements were calculated as [20]:

$$H_{ij} = \frac{1}{2}kS_{ij}(H_{ii} + H_{jj})$$

with the distance dependent weighted formula [21]

$$K = 1 + ke^{-\delta(R-R_o)} \quad with \quad k = \kappa + \Delta^2 - \kappa\Delta^4 \quad and \; \Delta = \frac{H_{ii} - H_{jj}}{H_{ii} + H_{jj}}$$

In these EHMO-ASED calculations the total potential energy E_{tot} is expressed as the sum of the electrostatic two-body correction E_{Rep} and the extended-Hückel binding energy DE_{EHMO}, as explained in [3] and [21]:

$$E_{tot}(R) = \Delta E_{EHMO}(R) + E_{Rep}(R)$$

A computer program to perform this type of calculations is available from the QCPE [22]. The parameters used are listed in Table 4 and were kept constant during all the calculations. The coulomb integrals H_{ii} were obtained by charge iteration on $HSi(OH)_3$, $CH_3Si(OH)_3$, and $ClSi(OH)_3$ at equilibrium geometry. Standard $\kappa = 1.0$ and $\delta = 0.35$ Å^{-1} were used with the exception of the Si–H, Si–C, and Si–Cl interactions for which $\kappa = 0.75$

Table 4.
EHMO parameters.

Atom	N	n_s	ζ_s	H_{ss} /eV	n_p	ζ_s	H_{pp} /eV
Si	4	3.000	1.7	-21.00	3.000	1.7	-12.840
O	6	2.000	2.575	-26.740	2.000	2.275	-11.260
C	4	2.000	1.625	-20.140	2.000	1.625	-11.240
Cl	7	3.000	2.183	-26.570	3.000	1.733	-14.780
H_{Si}	1	1.000	1.3	-14.390			
H_O	1	1.000	1.3	-15.50			
H_C	1	1.000	1.3	-13.690			

was used. Calculations have been carried out by assuming the following bond lengths and bond angles: d(Si–H) = 1.48 Å, d(Si–C) = 1.90 Å, d(Si–Cl) = 2.01 Å, d(Si–O) = 1.62 Å, d(C–H) = 1.09 Å, d(O–H) = 0.95 Å, a(Si–O–Si) = 148°, a(Si–O–H) = 117°, and tetrahedral angles for all four-coordinated centres.

Acknowledgement
This work is financed by the Schweizerischer Nationalfonds zur Förderung der wissenschaftlichen Forschung (project NF 20-34042.92) and by the Schweizerisches Bundesamt für Energiewirtschaft (project BEW-EPA 217.307).

REFERENCES

1. D.C. McKean and I. Torto, *Spectrochim. Acta, Part A* **49**, 1095 (1993) and references cited therein.
2. T.P.E. Auf der Heyde, H.-B. Bürgi, H. Bürgy, and Törnroos, *Chimia* **45**, 38 (1991).
3. G. Calzaferri and R. Hoffmann, *J. Chem. Soc., Dalton Trans.* 917 (1991).
4. a) P. Bornhauser and G. Calzaferri, *Spectrochim. Acta, Part A* **46**, 1045 (1990); b) M. Bärtsch, P. Bornhauser, H. Bürgy, and G. Calzaferri, *ibid.*, **47**, 1627 (1991); c) M. Bärtsch, P. Bornhauser, and G. Calzaferri, *SPIE* **1575**, 588 (1992).
5. M. Bärtsch, P. Bornhauser, G. Calzaferri, and R. Imhof, *J. Phys. Chem.* **98**, 2817 (1994).
6. A.L. Smith and N.C. Angelotti, *Spectrochim. Acta* **15**, 412 (1959).
7. H.-B. Bürgi, K.W. Törnroos, G. Calzaferri, and H. Bürgy, *Inorg. Chem.* **32**, 4914 (1993).
8. a) G. Calzaferri, R. Imhof, and K.W. Törnroos, *J. Chem. Soc., Dalton Trans.* 3123 (1994); b) G. Calzaferri, R. Imhof, and K.W. Törnroos *ibid.*, 3741(1993); c) G. Calzaferri and R. Imhof, *ibid.* 3391 (1992); d) G. Calzaferri, R. Imhof, and D. Herren, *Helv. Chim. Acta* **74**, 1228 (1991).
9. D. Herren, Ph.D. Thesis, Universität Bern, 1993.
10. M. Morán, C.M. Casado, I. Cuadrado, and J. Losada, *Organometallics* **12**, 4327 (1993).
11. M.D. Nyman, S.B. Desu, and C.H. Peng, *Chem. Mater.* **5**, 1636 (1993).
12. H. Kriegsmann, *Ber. Bunsen-Ges. Phys. Chem.* **65**, 336 (1961); H. Kriegsmann, *ibid.* **65**, 342 (1961).
13. T.A. Albright, J.K. Burdett, and M.H. Whangbo, *Orbital Interaction in Chemistry*, Wiley, New York, 1985.
14. P.A. Agaskar, *Inorg. Chem.* **30**, 2707 (1991).
15. K. Olsson, *Ark. Kemi* **13**, 367 (1958).
16. V.W. Day, W.G. Klemperer, V.V. Mainz, and D.M. Millar, *J. Am. Chem. Soc.* **107**, 8262 (1985).
17. H. Bürgy and G. Calzaferri, *J. Chromatogr.* **507**, 481 (1990).
18. R. Hoffmann, *J. Chem. Phys.* **39**, 1397 (1963).
19. R.S. Mulliken, *J. Phys. Chem.* **23**, 1833 (1955).
20. M. Wolfsberg and L. Helmholz, *J. Chem. Phys.* **29**, 837 (1952).
21. a) G. Calzaferri, L. Forss, and I. Kamber, *J. Phys. Chem.* **93**, 5366 (1989); b) M. Brändle and G. Calzaferri, *Helv. Chim. Acta* **76**, 924 (1993).
22. G. Calzaferri and M. Brändle, QCMP No. 116, *QCPE Bull.* **12***(4)*, (1992) update May (1993).